Ubiquitylation of the Bardet-Biedl syndrome protein complex is essential for cilium assembly and signaling

Francesco Chiuso et al.

Appendix Figures

Table of Contents

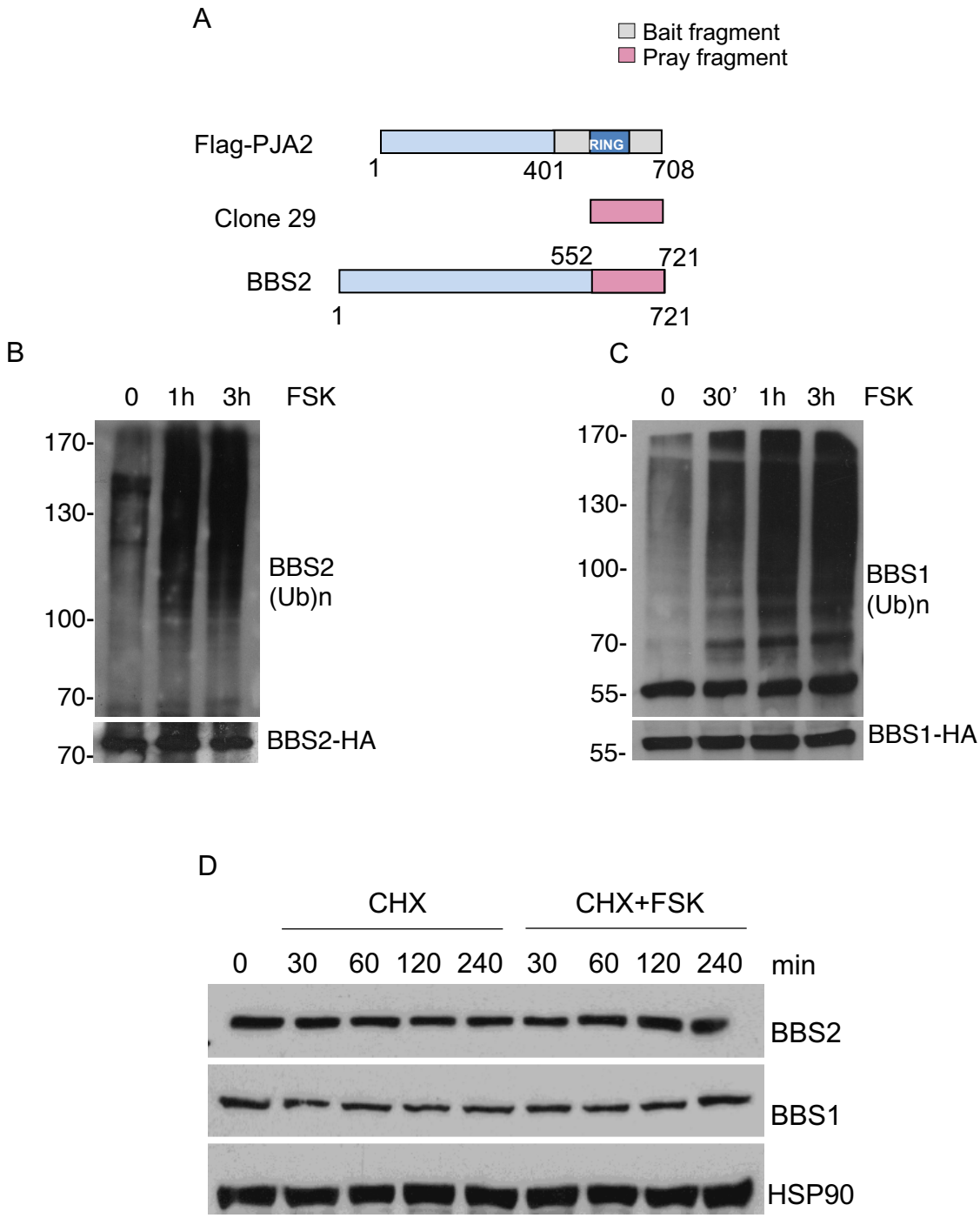

Appendix Figure S1. **A.** Schematic representation of human PJA2.The cysteine-rich region (RING) and the C-terminal rat clone 33 isolated by the yeast two-hybrid system are shown. Bait and pray fragment were indicated. **B,C** Immunoprecipitation of BBS2 (**B**) or BBS1 (**C**) from HEK293 cell lysates expressing HA-tagged BBS1 or BBS2 and ubiquitin-myc. Serum-deprived cells were left untreated or stimulated with FSK for 1 and 3 hours. Ubiquitinated BBS1 and BBS2 proteins and HA-tagged were detected. The precipitates were immunoblotted with anti-myc (ubiquitinated BBS1 or BBS2) and anti-HA antibodies. **D.** HEK293 cells were serum deprived for 24h, pretreated with cycloheximide (10μm) and stimulated with foskolin (40 μm) at indicated time. BBS1 and BBS2 protein levels were detected with endogenous antibody as indicated.

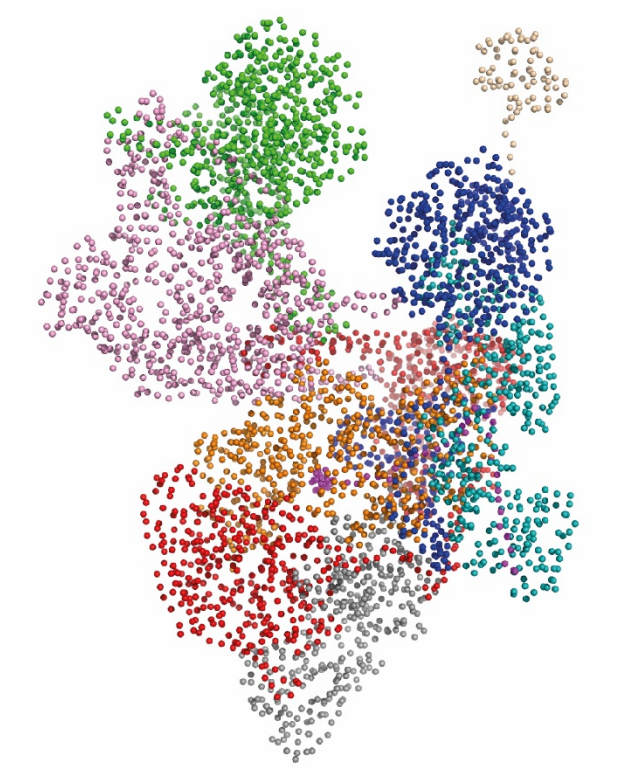

Appendix Figure S2: Coarse –Grained model of the Ub-hBBSome in an open conformation. Beads (BB) are shown as spheres.

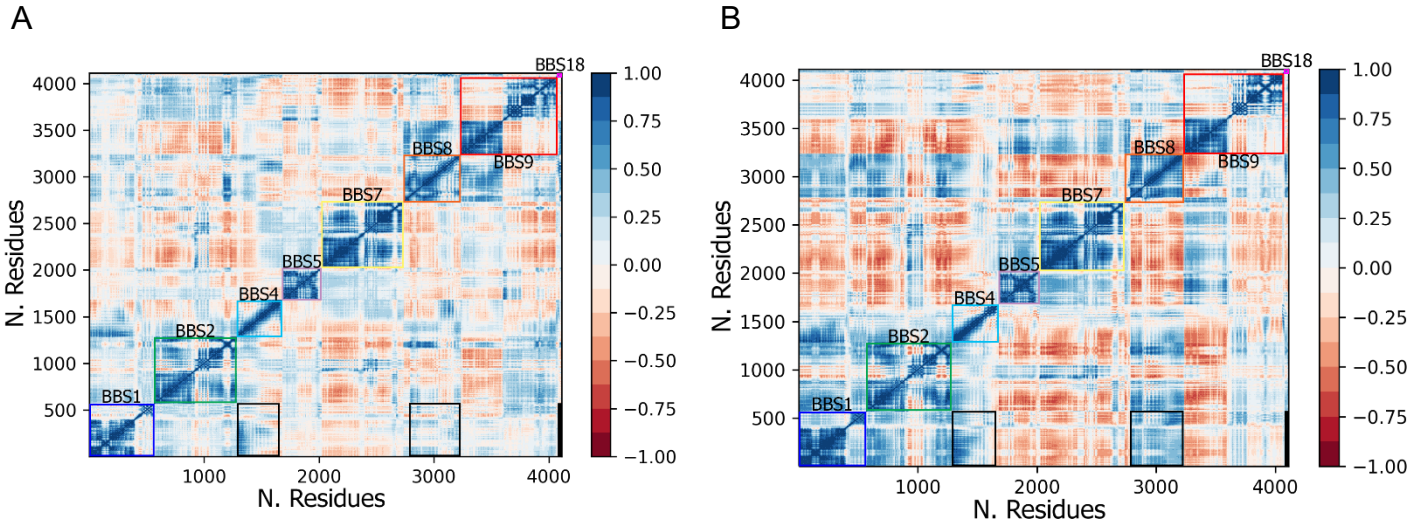

Appendix Figure S3: Atomic position Pearson Correlation Coefficient (aPCC) matrices calculated on **A** wt-hBBSome and **B** Ub-hBBSome after 5μs of CG-MD. Residues of each subunit are numbered as follows: BBS1 (S2-S568, blue rectangle),BBS2 (M570-V1285, green rectangle), BBS4 (F1288-L1683, cyan rectangle), BBS5 (M1685-S2025, light pink rectangle), BBS7 (M2026-A2740, yellow rectangle), BBS8 (M2742-F3239, orange rectangle), BBS9 (S3242-S4068, red rectangle), BBS18 (M4071-Q4122, purple rectangle). In particular, BBS18 presents a relatively high correlation (> 0.5) with BBS4 and BBS8, which is observed only in the Ub-hBBSome model. BBS18 also has high aPCC values with BBS1 and BBS2, which correlate with each other, too. BBS1 and BBS2 anticorrelate with BBS7 (aPCC < -0.5). The black rectangles highlight the zones showing high correlation between BB1, BBS4, BBS8 and BBS18 in Ub-hBBSome. The same areas are also highlighted in wt-hBBSome for the sake of comparison.

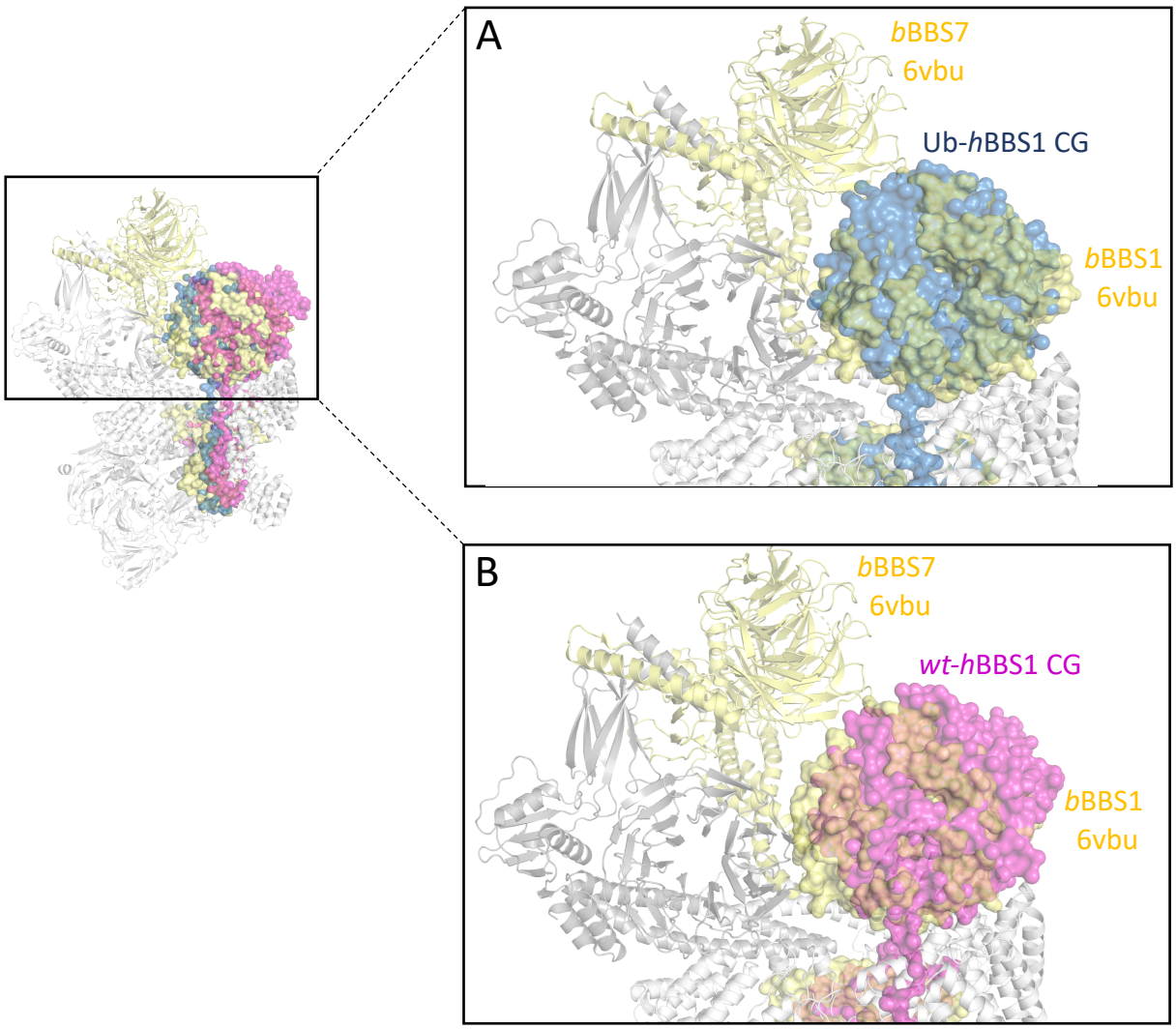

Appendix Figure S4: Superimposition between the bovine *b*BBS1 subunit of the apo (closed) form of the Cryo-EM *b*BBSome structure (PDB ID: 6vbu) (light-yellow surface) and the last CG-MD frame of: **A** CG model of the K143 Ubiquitinated *h*BBS1 (Ub-*h*BBS1 CG) (light-blue surface) and **B** CG model of the wild-type *h*BBS1 (wt-*h*BBS1 CG) (light-magenta surface). After 5 μs of CG-MD, a more closed conformation of the Ub-*h*BBS1 CG can be observed, compared to the wt-*h*BBS1 CG.

A

B

Appendix Figure S5

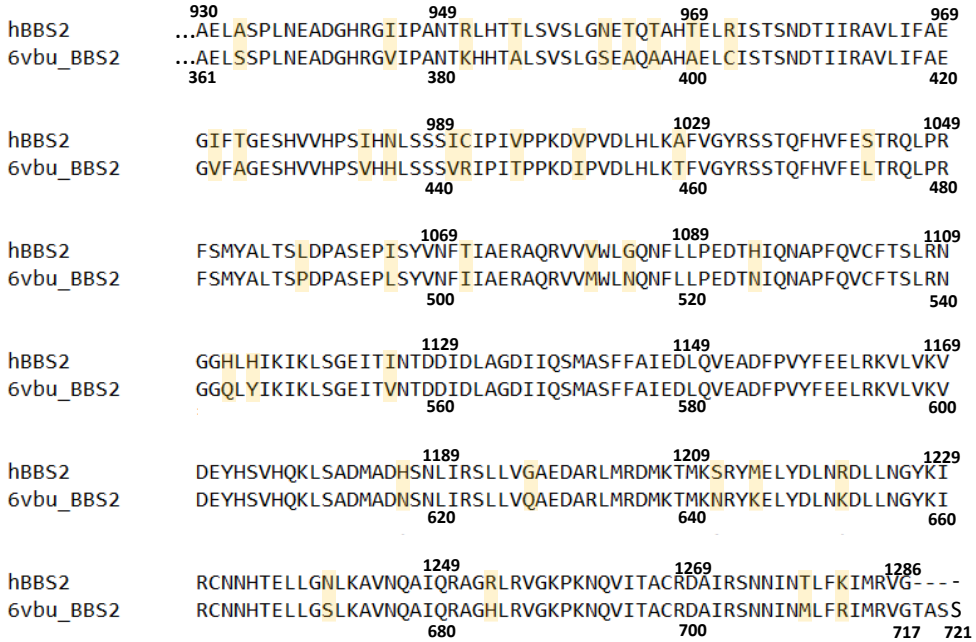

C

Appendix Figure S5

D

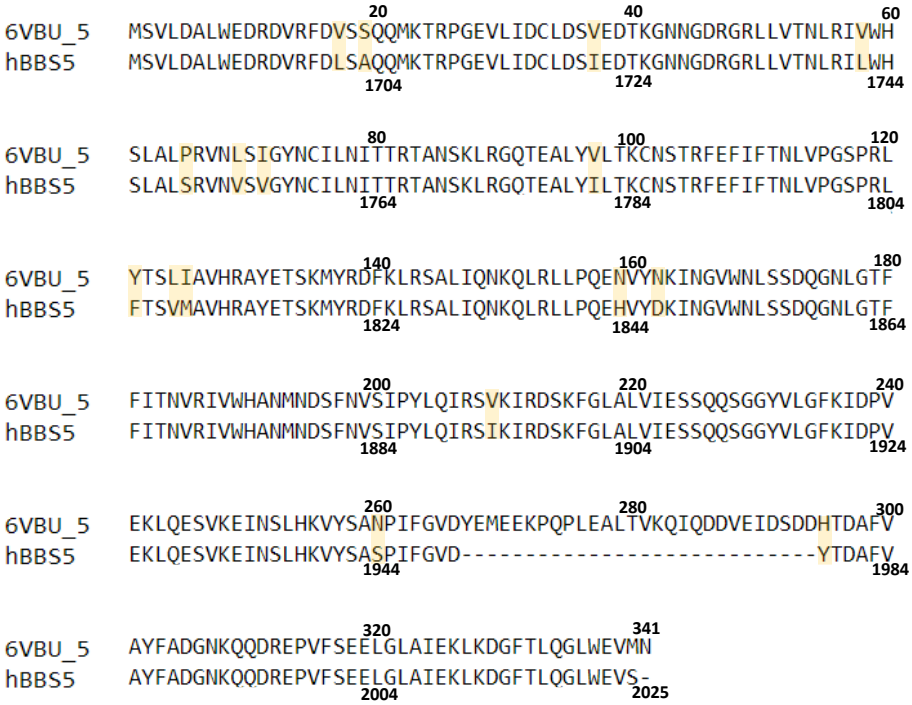

E

Appendix Figure S5

```
                                620                 640                 660
6VBU_7   SVKHTLKLIHPKLEYQLLLAKKVQLIDALKELQVHEGNTNFLIPEYRCILEEADHLQEEY
hBBS7    SVKHTLKLIHPKLEYQLLLAKKVQLIDALKELQIHEGNTNFLIPEYHCILEEADHLQEEY
                           2645                2665                2685

                680                 700                 715
6VBU_7   KKQPAHLERLYGMITDLFIDKFKFKGTNVKTKVPLLLEILDSYDQNALIAFFDAA
hBBS7    KKQPAHLERLYGMITDLFIDKFKFKGTNVKTKVPLLLEILDSYDQNALISFFDAA
                   2705                2725                2740
```

F

```
                 20                  40                  60
6VBU_BBS8  MEPLLLAWSYFRRRRFQLCADLCTQMLEKSPCDQAAWILKARALTEMVYVDEIDVDEEGI
hBBS8      MEPLLLAWSYFRRRKFQLCADLCTQMLEKSPYDQAAWILKARALTEMVYIDEIDVDQEGI
                   2760                2780                2800

                 80                  100                 120
6VBU_BBS8  AEMILDENAIAQVPRPGTSLKLPGTNQTGGPSPAVRPVTQAGRPITGFLRPSTQSGRPGT
hBBS8      AEMMLDENAIAQVPRPGTSLKLPGTNQTGGPSQAVRPITQAGRPITGFLRPSTQSGRPGT
                   2820                2840                2860

                 140                 160                 180
6VBU_BBS8  IEQAIKTPRTAYTARPIASSSGRFVRLGTASMLTSPDGPFINLSRLNLAKYAQKPKLAKA
hBBS8      MEQAIRTPRTAYTARPITSSSGRFVRLGTASMLTSPDGPFINLSRLNLTKYSQKPKLAKA
                   2880                2900                2920

                 200                 220                 240
6VBU_BBS8  LFEYIFHHENDVKTALDLAALSTEHSQYKDWWWKVQIGKCYYRLGLYREAEKQFKSALKQ
hBBS8      LFEYIFHHENDVKTALDLAALSTEHSQYKDWWWKVQIGKCYYRLGMYREAEKQFKSALKQ
                   2940                2960                2980

                 260                 280                 300
6VBU_BBS8  QEMVDTFLYLAKVYISLDQPLTALNLFKQGLDKFPGEVTLLCGIARIYEEMNNISSATEY
hBBS8      QEMVDTFLYLAKVYVSLDQPVTALNLFKQGLDKFPGEVTLLCGIARIYEEMNNMSSAAEY
                   3000                3020                3040

                 320                 340                 360
6VBU_BBS8  YKEVLKQDNTHVEAIACIGSNHFYTDQPEVALRFYRRLLQMGVYNCQLFNNLGLCCFYAQ
hBBS8      YKEVLKQDNTHVEAIACIGSNHFYSDQPEIALRFYRRLLQMGIYNGQLFNNLGLCCFYAQ
                   3060                3080                3100

                 380                 400                 420
6VBU_BBS8  QYDMTLTSFERALSLAENEEEVADVWYNLGHVAVGTGDTNLAHQCFRLALVSNNQHAEAY
hBBS8      QYDMTLTSFERALSLAENEEEAADVWYNLGHVAVGIGDTNLAHQCFRLALVNNNNHAEAY
                   3120                3140                3160

                 440                 460                 480
6VBU_BBS8  NNLAVLEMRRGHVEQAKALLQTASSLAPHMYEPHFNFATISDKIGDLQRSYAAAKKSEAA
hBBS8      NNLAVLEMRKGHVEQARALLQTASSLAPHMYEPHFNFATISDKIGDLQRSYVAAQKSEAA
                   3180                3200                3220

                 500
6VBU_BBS8  FPDHVDTQHLIKQLEQHFAML
hBBS8      FPDHVDTQHLIKQLRQHFA--
                   3240
```

G

```
                 20                  40                  60
6VBU_BBS9  MSLFKARDWWSTVLGDKEEFDQGCLCLADVDNTGNGQDKIIVGSFMGYLRIFNPHPVKTG
hBBS9      -SLFKARDWWSTILGDKEEFDQGCLCLANVDNSGNGQDKIIVGSFMGYLRIFSPHPAKTG
                   3260                3280                3300

                 80                  100                 120
6VBU_BBS9  DGAQAEDLLLEVHLRDPILQVEVGKFVSGTEMLHLAVLHSRKLCVYSVSGTLGNVEHGNQ
hBBS9      DGAQAEDLLLEVDLRDPVLQVEVGKFVSGTEMLHLAVLHSRKLCVYSVSGTLGNVEHGNQ
                   3320                3340                3360

                 140                 160                 180
6VBU_BBS9  YQIKLMYEHNLQRTACNMTYGSFGGVKGRDLICIQSVDGMLMVFEQESYAFGRFLPGSLL
hBBS9      CQMKLMYEHNLQRTACNMTYGSFGGVKGRDLICIQSMDGMLMVFEQESYAFGRFLPGFLL
                   3380                3400                3420

                 200                 220                 240
6VBU_BBS9  PGPLAYSSRTDSFITVSSCHQVESYKYQVLAFATDADKRQETEQQKHGSGKRLVVDWTLN
hBBS9      PGPLAYSSRTDSFLTVSSCQQVESYKYQVLAFATDADKRQETEQQKLGSGKRLVVDWTLN
                   3440                3460                3480

                 260                 280                 300
6VBU_BBS9  IGEQAIDICIVSFIQSASSVFVLGERNFFCLKDNGQIQFMKKLDYSPSCFLPYCSVSEGT
hBBS9      IGEQALDICIVSFNQSASSVFVLGERNFFCLKDNGQIRFMKKLDWSPSCFLPYCSVSEGT
                   3500                3520                3540

                 320                 340                 360
6VBU_BBS9  INTLIGNHNNMLHIYQDVTLKWATQLPHVPVAVRVGCLHDLKGVIVTLSDDGHLQCSYLG
hBBS9      INTLIGNHNNMLHIYQDVTLKWATQLPHIPVAVRVGCLHDLKGVIVTLSDDGHLQCSYLG
                   3560                3580                3600
```


Appendix Figure S5

H

Appendix Figure S5: BBSome bovine and human sequence alignments, highlighting the different residue numbers between the experimental (PDB ID: 6vbu) and the human homology model used during CG-MD simulations. **A.** *b*BBS1/*h*BBS1; **B**. *b*BBS2/*h*BBS2; **C**. *b*BBS4/*h*BBS4; **D**. *b*BBS5/*h*BBS5; **E**. *b*BBS7/*h*BBS7; **F**. *b*BBS8/*h*BBS8; **G**. *b*BBS9/*h*BBS9; **H**. *b*BBS18/*h*BBS18.

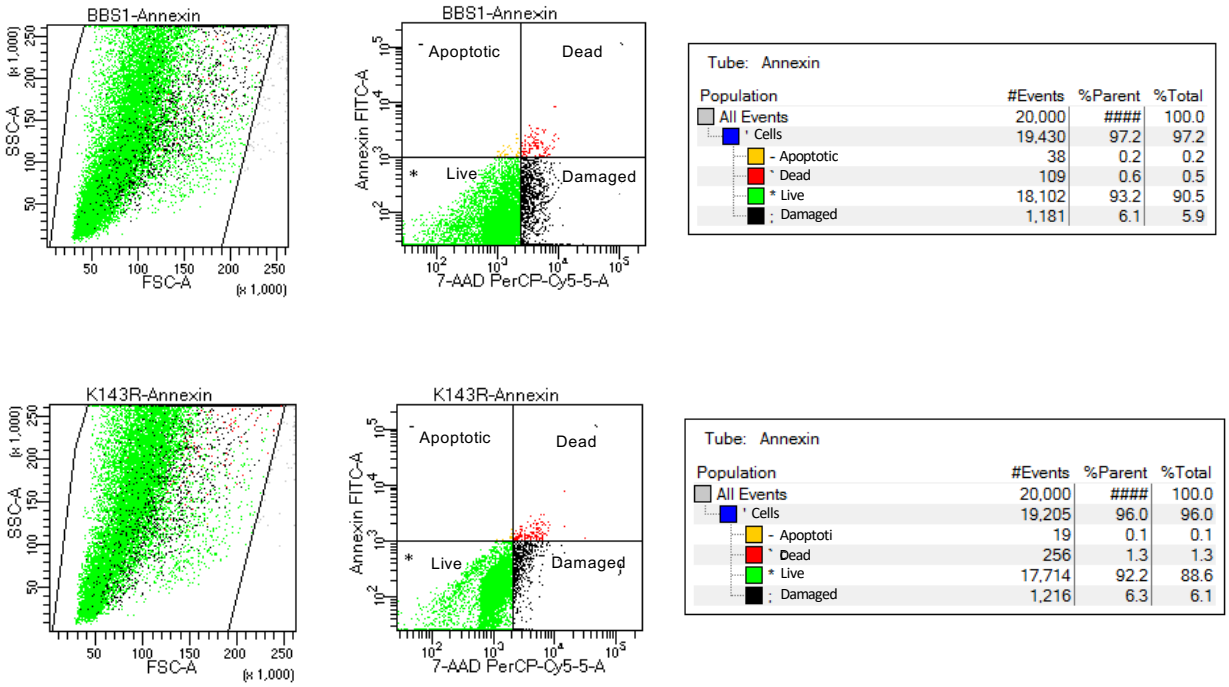

Appendix Figure S6: ARPE-19 cells were transiently transfected with Myc-tagged BBS1 variants or Myc-tagged BBS1- K143R. After 24h from transfection, cells were harvested and analyzed using a fluorescein isothiocynate (FITC) Annexin V Apoptosis Detection Kit and 7-AAD staining solution, according to the manufacturer's protocol.